NACA

RESEARCH MEMORANDUM

for the

U. S. Air Force

FREE-FLIGHT TESTS OF 0.11-SCALE NORTH AMERICAN F-100 AIRPLANE WINGS TO INVESTIGATE THE POSSIBILITY OF FLUTTER IN TRANSONIC SPEED RANGE AT VARYING ANGLES OF ATTACK

By Burke R. O'Kelly

Langley Aeronautical Laboratory
Langley Field, Va.

NATIONAL ADVISORY COMMITTEE
FOR AERONAUTICS

WASHINGTON

JUL 29 1954

NATIONAL ADVISORY COMMITTEE FOR AERONAUTICS

RESEARCH MEMORANDUM

for the

U. S. Air Force

FREE-FLIGHT TESTS OF 0.11-SCALE NORTH AMERICAN F-100 AIRPLANE WINGS TO INVESTIGATE THE POSSIBILITY OF FLUTTER IN TRANSONIC SPEED RANGE AT VARYING ANGLES OF ATTACK

By Burke R. O'Kelly

SUMMARY

Free-flight tests in the transonic speed range utilizing rocket-propelled models have been made on three pairs of 0.11-scale North American F-100 airplane wings having an aspect ratio of 3.47, a taper ratio of 0.308, 45° sweepback at the quarter-chord line, and thickness ratios of $3\frac{1}{2}$ and 5 percent to investigate the possibility of flutter. Data from tests of two other rocket-propelled models which accidentally fluttered during a drag investigation of the North American F-100 airplane are also presented.

The first set of wings (5 percent thick) was tested on a model which was disturbed in pitch by a moving tail and reached a maximum Mach number of 0.85. The wings encountered mild oscillations near the first-bending frequency at high lift coefficients. The second set of wings $\left(3\frac{1}{2}\right.$ percent thick$\left.\right)$ was tested up to a maximum Mach number of 0.95 at angles of attack provided by small rocket motors installed in the nose of the model. No oscillations resembling flutter were encountered during the coasting flight between separation from the booster and sustainer firing (Mach numbers from 0.86 to 0.82) or during the sustainer firing at accelerations of about 8g up to the maximum Mach number of the test (0.95). The third set of wings was similar to the first set and was tested up to a maximum Mach number of 1.24. A mild flutter at frequencies near the first-bending frequency of the wings was encountered between a Mach number of 1.15 and a Mach number of 1.06 during both accelerating and coasting flight. The two drag models, which were 0.11-scale models of the North American F-100 airplane configuration, reached a maximum Mach number of 1.77. The wings of these models had bending and torsional frequencies which were 40 and 89 percent, respectively, of the calculated scaled frequencies of the full-scale 7-percent-thick wing. Both models experienced flutter of the same type as that experienced by the third set of wings.

INTRODUCTION

At the request of the U. S. Air Force, free-flight rocket-propelled model tests at transonic speeds at varying angles of attack have been conducted to investigate the possibility of flutter of the 0.11-scale North American F-100 airplane wing and horizontal tail.

Calculations by the North American Aviation, Incorporated had shown that the F-100 airplane wing was subject to quasi-single-degree bending flutter over a Mach number range near 1.0. Tests utilizing rocket-propelled models were made to investigate this predicted flutter condition. This paper presents results of a series of five tests; three of which were flutter tests and two of which were drag model tests which encountered flutter.

The wings to be tested had thicknesses of 5 and $3\frac{1}{2}$ percent in order that both wing- and tail-surface flutter could be investigated. The North American F-100 airplane, as originally proposed, has a 7-percent-thick wing and tail, the tail surfaces being 0.49 scale of the wings. The test wings were purposely made weaker than the scaled values of the prototype. In this way, if the rocket model wings did not flutter, it would be expected that the full-scale wings would also be free of flutter. The 5-percent-thick wings, at sea level, had the mass ratio of the full-scale 7-percent-thick wings at 33,000 feet and the 7-percent-thick tail at 41,000 feet but had only 65 percent of the required scaled bending frequency. The $3\frac{1}{2}$ percent-thick wings, at sea level, had the mass ratio of the full-scale 7-percent-thick wings at 25,000 feet and the 7-percent-thick tail at 34,500 feet but had only 45.5 percent of the required scaled bending frequency.

As a part of the test program, two 0.11-scale rocket-powered models of the North American F-100 airplane were tested to determine the drag characteristics (ref. 1) and the results from these tests which pertain to flutter are included in this report. The wings of these models were not, however, dynamically scaled. The bending and torsional frequencies of these 7-percent-thick wings were 40 and 89 percent, respectively, of the calculated scaled frequencies of the full-scale 7-percent-thick wing.

SYMBOLS

A_{ex} aspect ratio of exposed wing panels

a_n/g normal accelerometer reading

$a + x_\alpha$ location of center of gravity of wing section from midchord, positive rearward, $\frac{\text{Twice percent chord}}{100} - 1$

b semichord of test wing normal to quarter-chord line, ft

c local wing chord, free stream, in.

f frequency, cps

g acceleration due to gravity, ft/sec^2

I_α polar mass moment of inertia about the elastic axis per unit length, $ft\text{-}lb\text{-}sec^2/ft$

M Mach number

m mass of wing per unit length, slugs/ft

r_{cg}^2 square of nondimensional radius of gyration about the center of gravity, I_α/mb^2

S_{ex} wing area of two exposed wing panels, sq ft

t flight time from launching, sec

V velocity, fps

W/S wing loading, lb/sq ft

Λ sweepback at quarter-chord line, deg

λ taper ratio of exposed wing panel, c_t/c_r

μ mass ratio, $m/\pi\rho b^2$

ρ atmospheric density, $slugs/ft^3$

Subscripts:

h_1 first bending

h_2 second bending

std standard conditions

α_1 first torsion

MODELS AND INSTRUMENTATION

Models

The flutter models tested consisted of two types. The first type was basically the same as that described in reference 2 with the exception of a moving tail and the associated mechanism. The tail fins had a modified double-wedge airfoil section. The mechanism consisted of an electric motor coupled to reduction gears which drove a cam-fork arrangement connected to a control rod attached to the tail. This arrangement resulted in the tail moving sinusoidally with respect to time. By changing gears and adjusting the linkages, the rate of pulsing and the amount of deflection could be selected prior to the flight. A sketch of this type of rocket-propelled flutter model with the dynamically scaled flutter wings attached may be seen in figure 1(a) and a photograph is shown in figure 2(a). The second type of flutter test vehicle has been described in reference 2 and a sketch of this type with the flutter wings attached is shown in figure 1(b). A photograph may be seen in figure 2(b). Two small rocket motors were installed in the nose of this model to disturb the model in pitch. These flutter models used the same type of booster so that the models were accelerated to about $M = 0.8$. After separation from the booster, a five-inch cordite rocket motor incorporated in each model as a sustainer accelerated the model at about 8g to the maximum Mach number of the test.

The two drag models, which were 0.11-scale models of the North American F-100 airplane with and without horizontal-tail surfaces, have been previously described in reference 1.

Weight and balance data for both the flutter models and the drag investigation models are presented in table I.

Test Wings

Three pairs of flutter wings were tested in this investigation. In plan form, the wings were identical. The wings of models 1 and 3, however, were 5 percent thick and the wings for model 2 were $3\frac{1}{2}$ percent thick These wings were made of solid magnesium alloy and when mounted on the test vehicle were swept back 45° at the quarter-chord line with a taper ratio of 0.308, an aspect ratio of 3.47, and NACA 64A series airfoil

sections modified from the 70-percent-chord station to the trailing edge for ease of machining. Figure 3 shows a sketch of the wing and the root attachment. Structural characteristics and natural frequencies of the wings found by vibrating the wings while attached to the body are given in table II. Structural influence coefficients were taken for the wings. Figure 4 is a sketch of the wings showing the points of load application and deflection measurements and the wing panels for which the masses were determined for use with the structural influence coefficients. For the determination of the influence coefficients, each wing was loaded by means of a weighted frame which could be slipped over the wing in such a manner that a point load could be applied. The deflections were measured with dial gages which could be read directly to 0.0001 inch. Tables III and IV give the values of the influence coefficients for both the 5- and the $3\frac{1}{2}$-percent-thick wings and the masses of the wing panels associated with the influence coefficients.

The wings of the drag models were fabricated of an aluminum-alloy spar with laminated-mahogany leading and trailing edges (fig. 3). Except for both pairs of these wings being 7 percent thick, they were dimensionally very nearly the same as the flutter wings although they were not dynamic models. The two sets of wings had the same vibration characteristics, that is, the natural frequencies and the node lines were the same.

Figure 5 shows the node lines and frequencies of the wings of each model as determined by ground vibration tests with the wings mounted on the models.

A comparison of the first-bending and uncoupled-torsion frequencies of each of the models with the calculated scaled frequencies of the full-scale wings is given in the following table:

Frequency	Scaled airplane wings, 7-percent-thick	Flutter model 1	Flutter model 2	Flutter model 3	Drag models 1 and 2
f_{h_1}	78.6	50	34	49	31
f_{α_1}	287.4	313	198	294	256

Instrumentation

The models were equipped with multichannel telemeters which gave continuous records of the quantities to be measured; namely, torsion

and bending strains for each of the wings, total pressure, normal acceleration near the model center of gravity, angle of attack, and, with the exception of model 2, position of the tail. In model 3, one of the wing torsion gages was inoperative. The strain gages were located on the wing so that the bending gages were practically insensitive to torsional strain, but the torsion gages could not be made insensitive to bending strain.

The instrumentation for the drag models is described in reference 1. A normal accelerometer located in the wing root about 5 inches outboard of the model center line was used to detect any wing vibrations.

Atmospheric conditions prevailing at the times of the flights were obtained from radiosondes. The radiosonde was tracked by radar to determine wind direction and velocity up to the maximum altitudes of the models. Two radar sets tracked the models during the flights; one to give the velocity of the models with respect to a ground reference point and the other to give their position in space. All the flights were tracked by motion-picture cameras to give photographic records of the flights.

The models were launched at the Langley Pilotless Aircraft Research Station at Wallops Island, Va.

PRESENTATION OF RESULTS

Model 1 (5-percent-thick wings).- A time history of the flight of model 1 showing Mach number, velocity, and atmospheric density is shown in figure 6(a). A portion of one of the telemeter records is reproduced in figure 7(a) and a reduction of the data from the telemeter record is shown in figure 8(a).

The angles of attack and normal accelerations reached rather high values when the model responded to the pulsed tail (fig. 7(a)) and because of this, the tail fins were overloaded and broke off and thus caused the model to become unstable. Consequently, the model broke in two and the useful portion of the flight was terminated.

The tail was pulsed sinusoidally from a zero position to -10° at the rate of 3 cycles per second. The angle-of-attack response to this pitch disturbance reached values as high as 13.4° and -6.6° and the normal accelerations reached values as high as 23g and -10g. At the time of the model breakup, the angle of attack was in excess of 14.8° and the normal acceleration was in excess of 27.5g, these values being the instrument limits. The Mach number at this time was 0.83, the maximum attained in the test. Motion pictures of the flight showed that neither of the wings broke off of the model even at the high angles of attack.

During these oscillations, the wing strain gages showed the wings to be bending but not twisting and no violent flutter was evident even at the high angles of attack. The small deflections shown by the torsion gages are due primarily to the wing bending. The bending strain gages (fig. 7(a)) show a low-amplitude oscillation of approximately 50 cycles per second at 1.9 seconds (M = 0.74) on the right wing and about 73 cycles per second at 2.3 seconds (M = 0.79) on the left wing. These oscillations occur primarily at high lift coefficients and they may be the result of wing motion in the wing-bending flutter mode or of flow separation.

Model 2 ($3\frac{1}{2}$-percent-thick wings).- A time history of the flight of model 2 showing Mach number, velocity, and atmospheric density is shown in figure 6(b). A reduction of the data from the telemeter record from launching to model breakup is shown in figure 8(b).

At $M \approx 0.94$, the first disturbing rocket fired caused the model to pitch up so that it reached an angle of attack in excess of 10° and a normal acceleration in excess of 23g, these values being the instrument limits (fig. 8(b)). These high values, apparently due to disturbing rocket malfunction, again created an overload on the tail fins which failed and caused the model to become unstable. The model, however, did not break apart even though the useful portion of the flight was terminated. The strain gages indicated that the wings were bending and twisting rather large amounts. The maximum Mach number of the test was M = 0.95. Motion pictures showed that neither wing broke off of the model during the flight. There were no wing oscillations during the coasting flight between separation of the model from the booster and sustainer firing; this coasting flight was in the Mach number range 0.86 to 0.82 where the wings of the first model oscillated under a longitudinal acceleration of 8g. There were no wing oscillations similar to flutter during sustainer firing, where the longitudinal acceleration of the model was about 8g, up to the maximum Mach number of the test.

Model 3 (5-percent-thick wings).- Model 3 had a relatively low altitude flight and a time history of this flight showing Mach number, velocity, and atmospheric density is shown in figure 6(c). A portion of one of the telemeter records is reproduced in figure 7(b) and a reduction of the data from the telemeter record is shown in figure 8(c).

The tail was pulsed sinusoidally from a zero position to -5° at the rate of $2\frac{1}{2}$ cycles per second. The angle of attack on the first pulse ranged from 5.3° to -0.7°. These maximum values gradually decreased in magnitude with each suceeding pulse as the Mach number increased to the maximum value (fig. 8(c)). The normal acceleration varied from 8g to -3g. The maximum Mach number attained in the test was M = 1.24. No violent flutter occurred over the speed range experienced in the test. However, the two bending strain gages (fig. 7(b)) show a low-amplitude undamped

oscillation of approximately 62 cycles per second at 4.5 seconds (M = 1.15) during the accelerating portion of the flight and again at 7.3 seconds (M = 1.06) during the decelerating portion of the flight. These same oscillations occur at other times during the flight but are not as sustained as at these times. These oscillations appear to be in the wing first-bending flutter mode as the first-bending frequency of the wings in still air was 49.0 cycles per second and no motion of like nature was indicated on the torsion strain gage.

Drag model 1.- A time history of the flight of drag model 1 showing Mach number, velocity, and atmospheric density during that portion of the decelerating flight in which flutter occurred is shown in figure 6(d), and a portion of one of the telemeter records showing the flutter oscillations is presented in figure 7(c). These oscillations occurred between the Mach numbers of 0.94 and 1.11 at a frequency of 50 cycles per second. The first-bending frequency of the wings was 31 cycles per second and the first torsional frequency was 256 cycles per second. The double amplitude of the oscillations was about 0.3g as measured by a normal accelerometer located in the wing root. A study of these figures indicates strongly that the wings encountered essentially the same type of oscillations as at least one of the flutter models.

Drag model 2.- Figure 6(e) shows a time history of this flight during the decelerating portion when flutter occurred and presents Mach number, velocity, and atmospheric density. Figure 7(d) is a reproduction of a portion of the telemeter record which shows the flutter oscillations. These oscillations occurred at about the same Mach number range (0.94 to 1.1) as did those of the first drag model and at the same frequency (50 cycles per second). The first-bending frequency of these wings was 31 cycles per second; the first-torsional frequency was 256 cycles per second; and the double amplitude of the flutter was again about 0.3g measured in the same way. It appears evident that these wings experienced the same type of flutter as the wings of the other drag model and essentially the same as one of the flutter models.

CONCLUDING REMARKS

Free-flight rocket-propelled models with 0.11-scale wings of the North American F-100 airplane of different thicknesses have been tested at varying angles of attack. One flutter model having 5-percent-thick wings experienced mild wing oscillations at high lift coefficients over a Mach number range of 0.71 to 0.80 at frequencies of 50 and 73 cycles per second. These oscillations may be the result of wing motions in the bending flutter mode or of flow separation. A flutter model having $3\frac{1}{2}$-percent-thick wings did not experience any wing oscillations over a

Mach number range of 0.86 to 0.82 as did one of the other models. This speed range was during decelerating flight between separation of the model from the booster and sustainer firing. During the sustainer firing at an acceleration of about 8g, the wings were also free of flutter up to the maximum Mach number of 0.95. (Another set of 5-percent-thick flutter wings fluttered sporadically over a Mach number range of 0.90 to 1.24 at a frequency of about 62 cycles per second.)

Two drag-investigation models having 7-percent-thick wings encountered the same type of flutter as the third flutter model over a Mach number range of about 1.10 to 0.94 at a frequency of 50 cycles per second.

The oscillations and flutter which were encountered by four of the five models tested would probably not occur on the full-scale airplane wings because of the large differences in the wing stiffnesses between the model wings and the full-scale wings and because the structural damping of the full-scale wing of rib and spar construction would be higher than the structural damping of the two types of model wings of solid material and solid spar and fairing construction.

Langley Aeronautical Laboratory,
National Advisory Committee for Aeronautics,
Langley Field, Va., July 14, 1954.

David B. Stone
for Burke R. O'Kelly
Aeronautical Research Scientist

Approved: Joseph A. Shortal
Joseph A. Shortal
Chief of Pilotless Aircraft Research Division

DY

REFERENCES

1. Blanchard, Willard S., Jr.: A Summary of the Drag and Longitudinal Trim at Low Lift of the North American YF-100A Airplane at Mach Numbers From 0.75 to 1.77 As Determined by Flight Tests of 0.11-Scale Rocket Models. NACA RM SL54B01, U. S. Air Force, 1954.

2. Lauten, W. T., Jr., and O'Kelly, Burke R.: Results of Two Experiments on Flutter of High-Aspect-Ratio Swept Wings in the Transonic Speed Range. NACA RM L52D24b, 1952.

TABLE I

WEIGHT AND BALANCE DATA OF MODELS

	Flutter models			Drag models	
	1	2	3	1	2
Weight with fuel, lb	156.5	133.5	156.25	167.5	169.8
Weight without fuel, lb	128.0	105.5	128.75	149.5	151.8
Wing loading with fuel, lb/sq ft	44.7	38.2	44.7	47.3	48.0
Wing loading without fuel, lb/sq ft	36.6	30.2	36.6	42.3	43.0
Center of gravity with fuel, in.	52.88	52.75	52.68	34.99	34.63
Center of gravity without fuel, in.	50.06	50.96	50.00	34.99	34.56

TABLE II

WING CHARACTERISTICS AND

NATURAL FREQUENCIES

Model	r_{cg}^2 (calculated)	Center of gravity of wing section (calculated), percent c	μ_{std} (calculated)	$a + x_\alpha$ (calculated)	f_{h_1}, cps	f_{h_2}, cps	f_{α_1}, cps	f_{h_1}/f_α	Sex, sq ft	Weight per exposed panel, lb	A_{ex}
Flutter model 1	0.2141	46.9	95.5	-0.062	50.0	173	313	0.16	3.50	7.28	3.14
Flutter model 2	0.2098	46.9	66.3	-0.062	34	129	198	0.172	3.50	5.34	3.14
Flutter model 3	0.2141	46.9	95.5	-0.062	49.0	180.5	294	0.166	3.50	7.34	3.14
Drag models	0.1881	43.6	97.9	-0.128	31	101	256	0.121	3.54	----	3.12

TABLE III

STRUCTURAL INFLUENCE COEFFICIENTS

FOR STATIONS SHOWN IN FIGURE 4

(a) Model 1.* 5-percent-thick wings; 25-pound load

Load at station -	Deflection in inches at station -											
	1	2	3	4	5	6	7	8	9	10	11	12
1	912×10^{-4}	461×10^{-4}	156×10^{-4}	34×10^{-4}	4×10^{-4}	1092×10^{-4}	660×10^{-4}	250×10^{-4}	76×10^{-4}	357×10^{-4}	137×10^{-4}	17×10^{-4}
2	454	284	109	27	3	512	349	159	54	214	90	12
3	159	113	64	21	3	164	117	73	32	79	38	6
4	32	26	20	12	3	35	25	19	10	16	8	2
5	2	2	3	3	1	3	3	3	1	2	1	1
6	1084	509	162	32	3	1486	830	283	81	442	166	19
7	653	350	110	22	1	827	558	207	61	325	130	15
8	244	161	67	18	2	288	208	107	38	143	70	9
9	74	56	28	11	1	91	66	39	17	45	27	5
10	347	212	73	15	1	433	319	140	44	234	101	12
11	130	89	35	8	0	163	123	66	24	97	67	8
12	17	12	5	2	0	19	14	8	5	11	8	3

*Models 1 and 3 were essentially the same.

TABLE III.- Concluded

STRUCTURAL INFLUENCE COEFFICIENTS

FOR STATIONS SHOWN IN FIGURE 4

(b) Model 2. $3\frac{1}{2}$-percent-thick wings; 25-pound load

Load at station -	Deflection in inches at station -														
	1	2	3	4	5	6	7	8	9	10	11	12	13	14	15
1	1950×10^{-4}	958×10^{-4}	333×10^{-4}	59×10^{-4}	0×10^{-4}	2176×10^{-4}	1234×10^{-4}	545×10^{-4}	157×10^{-4}	12×10^{-4}	2385×10^{-4}	1504×10^{-4}	769×10^{-4}	283×10^{-4}	35×10^{-4}
2	942	585	231	47	0	1016	675	347	110	10	1089	767	449	181	24
3	327	234	135	35	1	342	245	151	660	7	347	253	160	76	9
4	49	44	30	19	1	48	38	27	15	3	49	35	24	12	2
5	0	1	1	1	1	0	0	1	0	0	0	0	0	0	0
6	2183	1027	342	57	0	2584	1391	547	168	13	2966	1806	907	332	41
7	1244	675	246	44	0	1403	880	417	124	10	1552	1080	614	238	31
8	551	349	153	31	0	602	418	235	80	7	642	481	313	147	20
9	157	110	59	17	0	154	112	73	33	3	182	140	97	53	10
10	13	10	7	3	1	5	6	5	3	1	6	6	5	2	0
11	2405	1090	349	54	0	2989	1543	646	176	12	3646	2107	1038	376	47
12	1515	761	252	38	0	1823	1079	485	137	9	2121	1484	789	301	39
13	786	457	169	27	0	908	613	319	96	8	1034	787	535	224	30
14	277	177	72	12	0	325	237	145	52	4	376	300	226	148	23
15	35	25	8	2	0	40	30	20	10	1	43	34	29	21	12

TABLE IV

MASS OF NUMBERED PANELS OF WINGS

Panel designation (see fig. 4)	Model 1* mass, slugs	Model 2 mass, slugs
1	7.8898×10^{-4}	3.201×10^{-4}
2	13.8275	5.596
3	12.3988	8.647
4	17.7523	12.363
5	40.9398	16.779
6	5.6963	4.290
7	9.5346	7.502
8	16.6992	11.591
9	23.5690	16.573
10	7.0172	22.500
11	10.0470	1.849
12	28.6616	3.232
13	-------	4.994
14	-------	7.141
15	-------	9.695

*Models 1 and 3 were essentially the same.

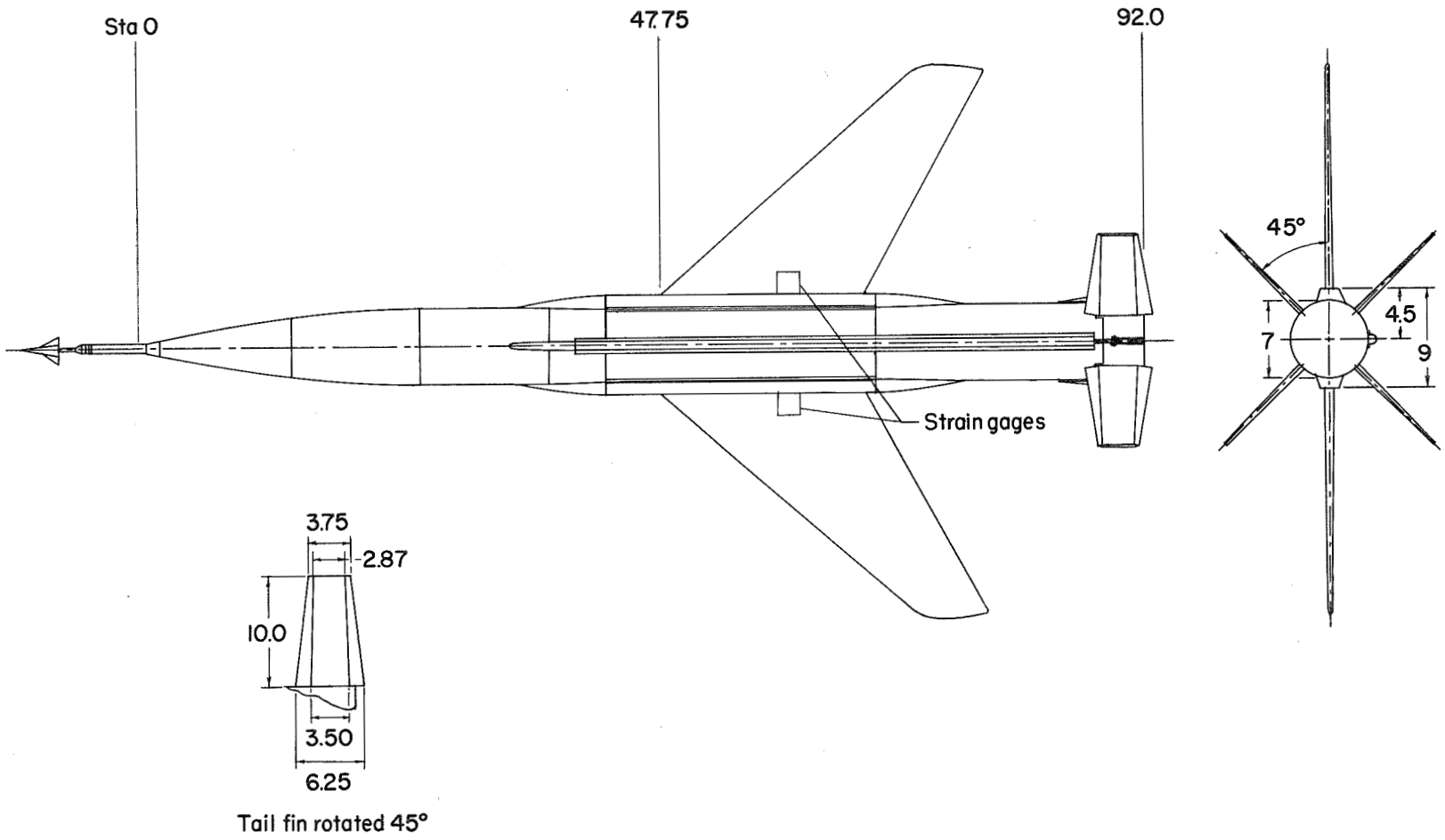

(a) Flutter models 1 and 3.

Figure 1.- Sketches of the models. All dimensions are in inches.

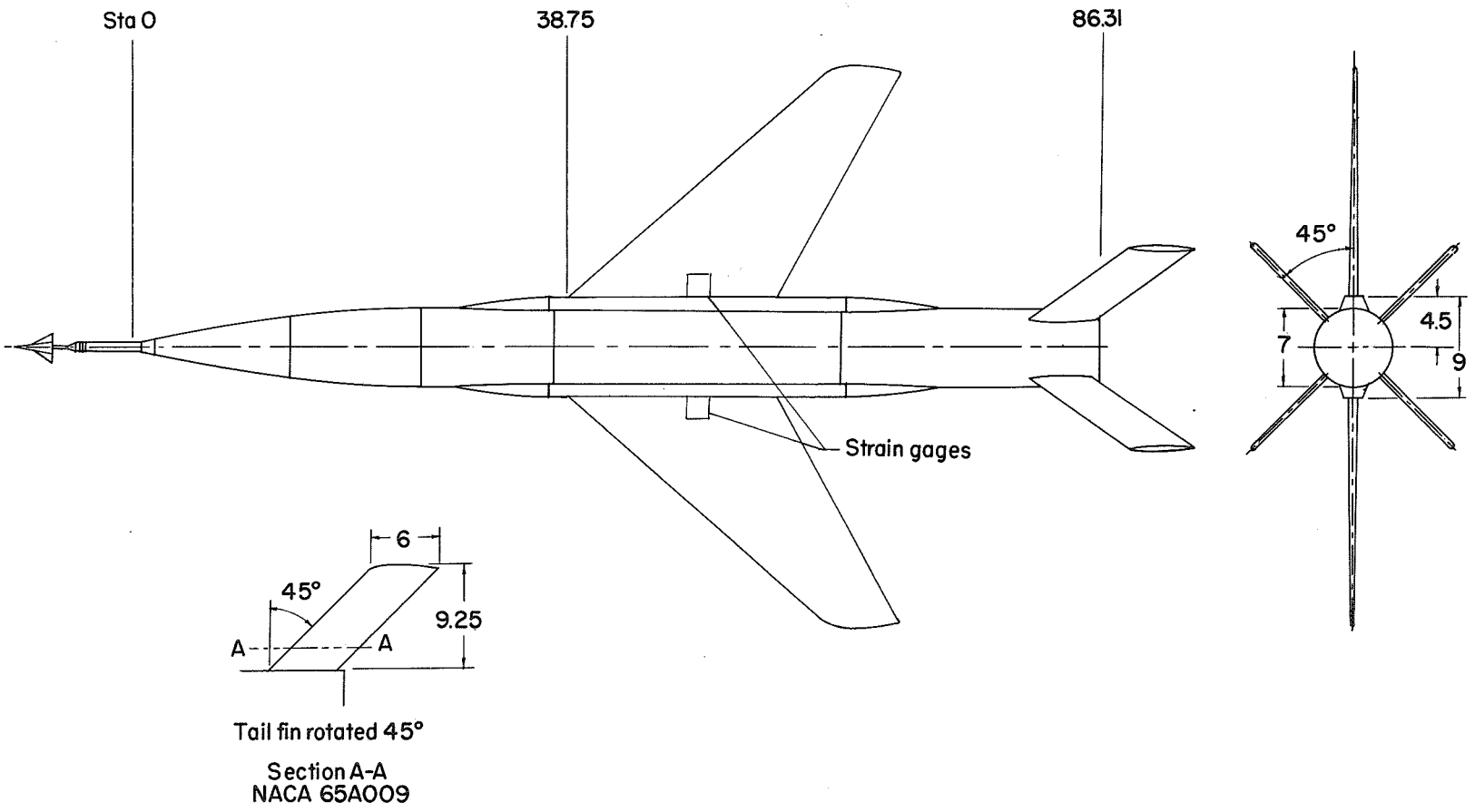

(b) Flutter model 2.

Figure 1.- Concluded.

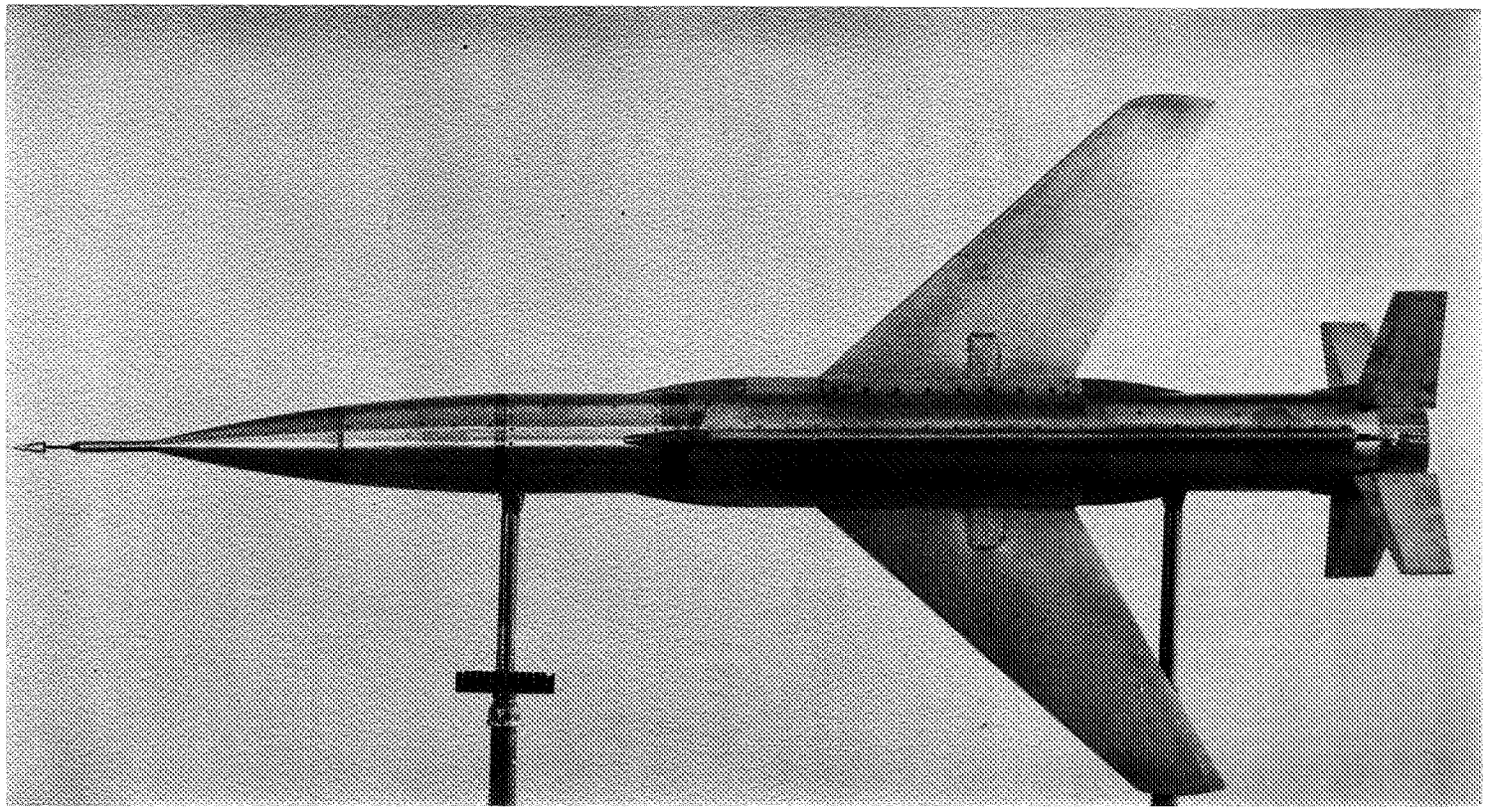

L-81110.1

(a) Moving-tail flutter model (models 1 and 3).

Figure 2.- Photographs of the models.

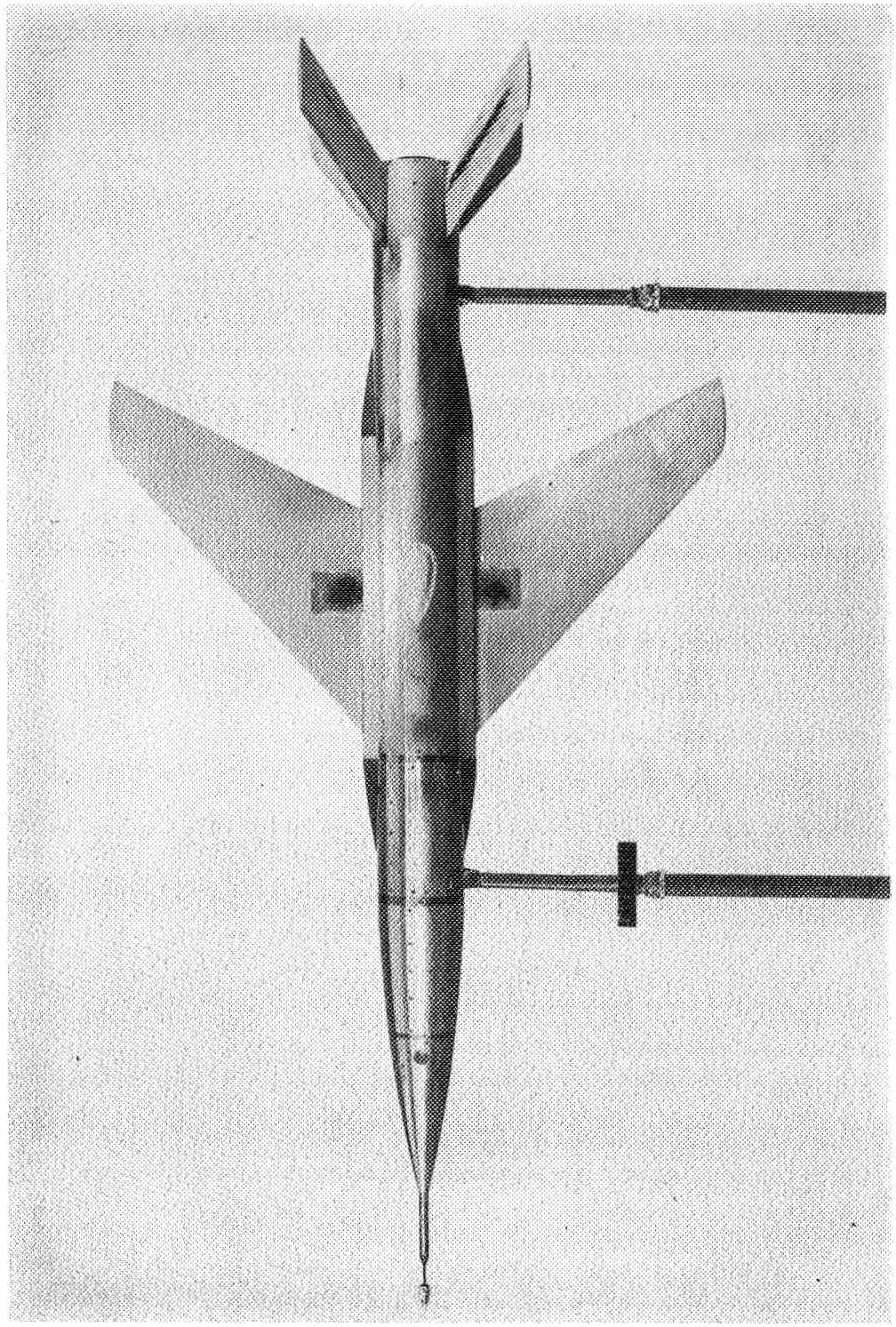

L-80940.1

(b) Fixed-tail model (model 2).

Figure 2.- Concluded.

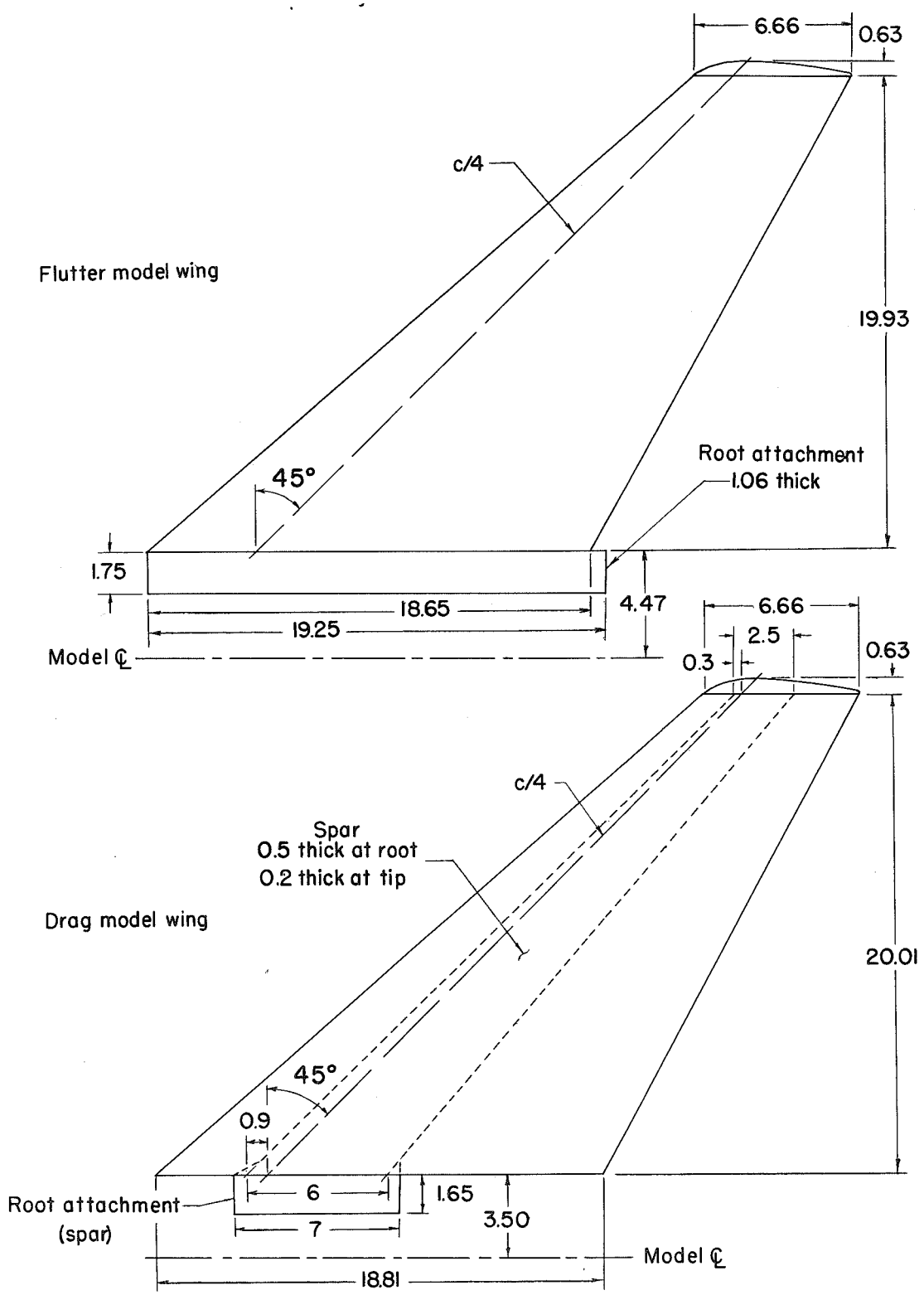

Figure 3.- Sketch of the wings. All dimensions are in inches.

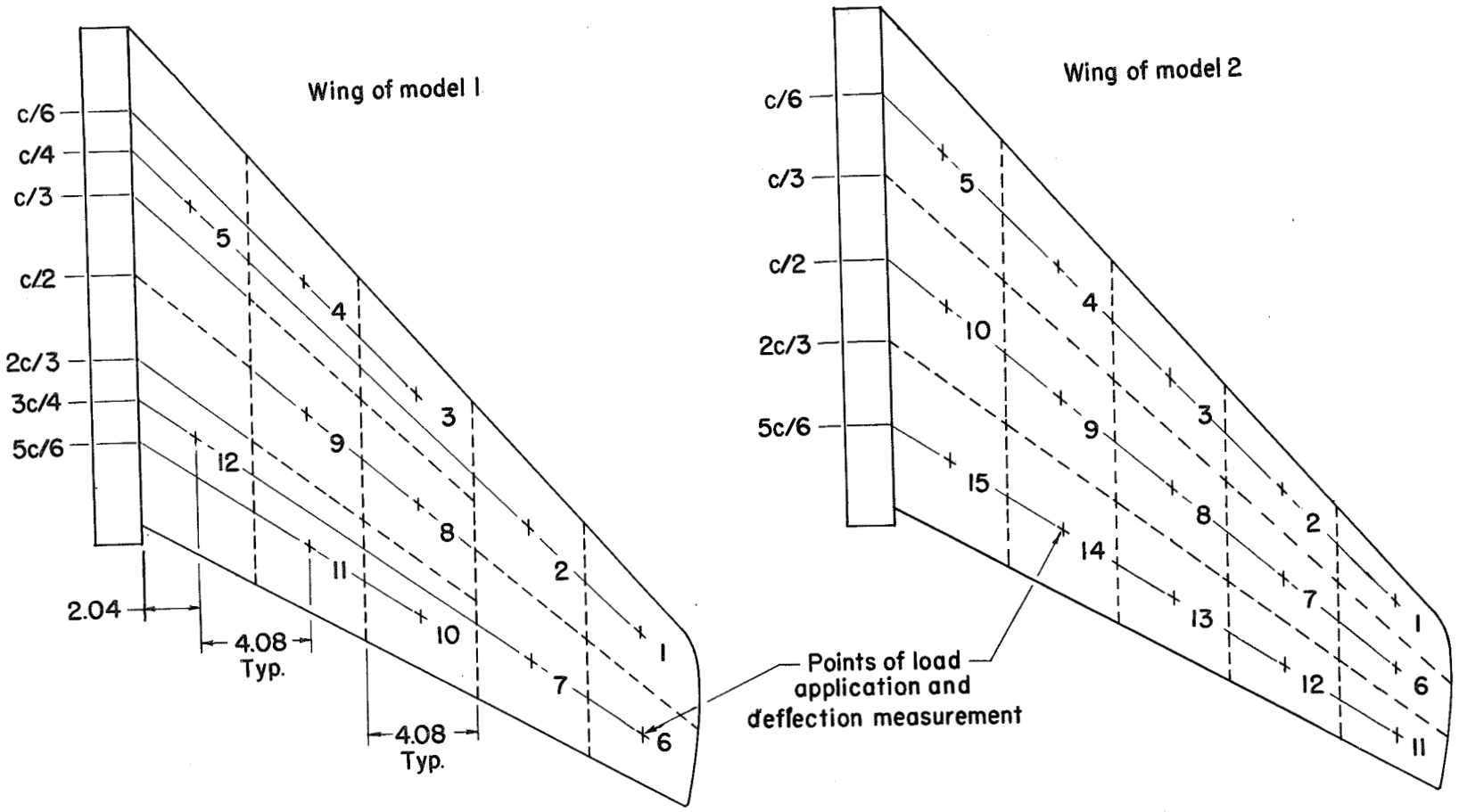

Figure 4.- Sketch designating wing-panel numbers and loading and measuring points. All dimensions are in inches.

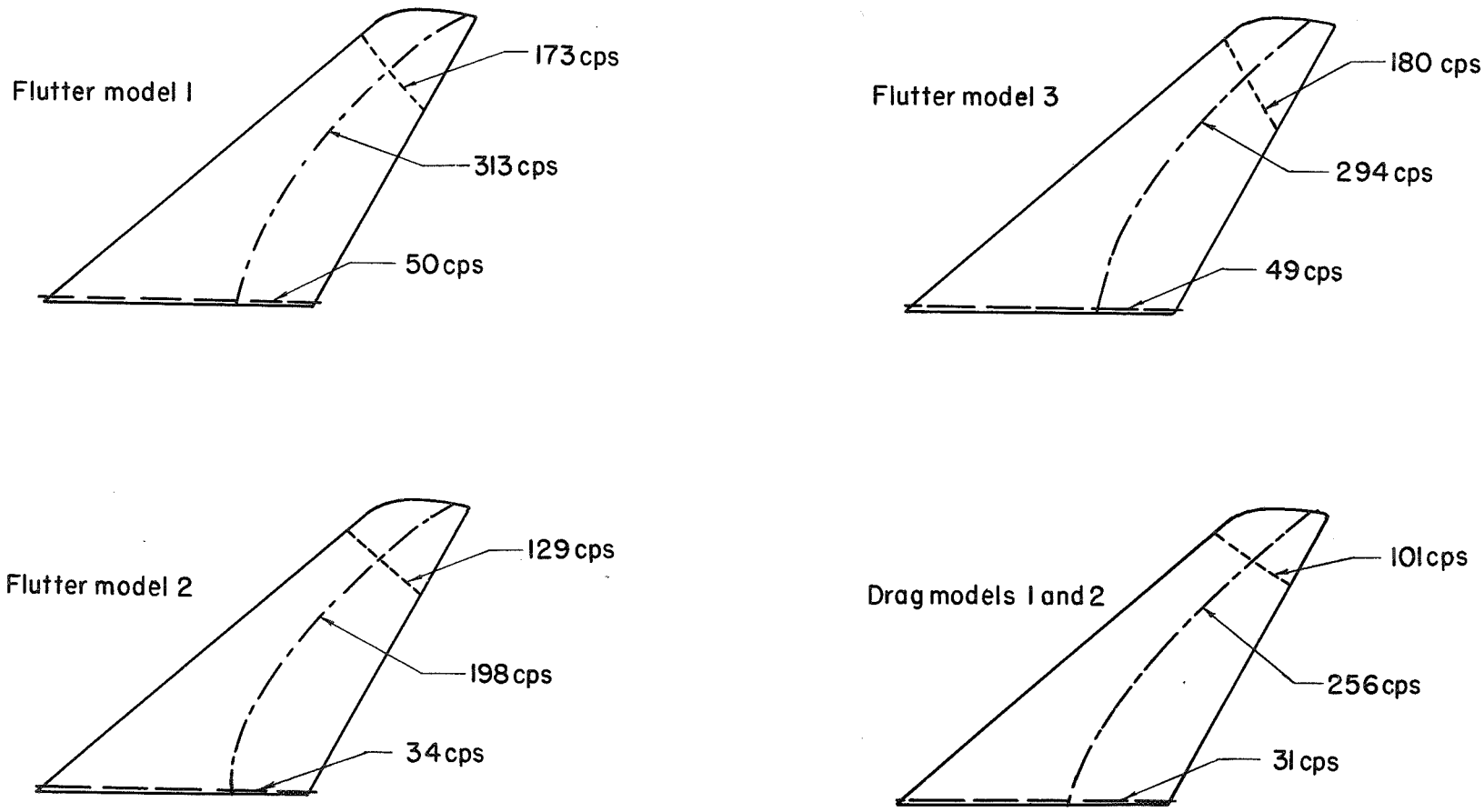

Figure 5.- Node lines and natural frequencies of the wings. Wings and node line locations are drawn to scale.

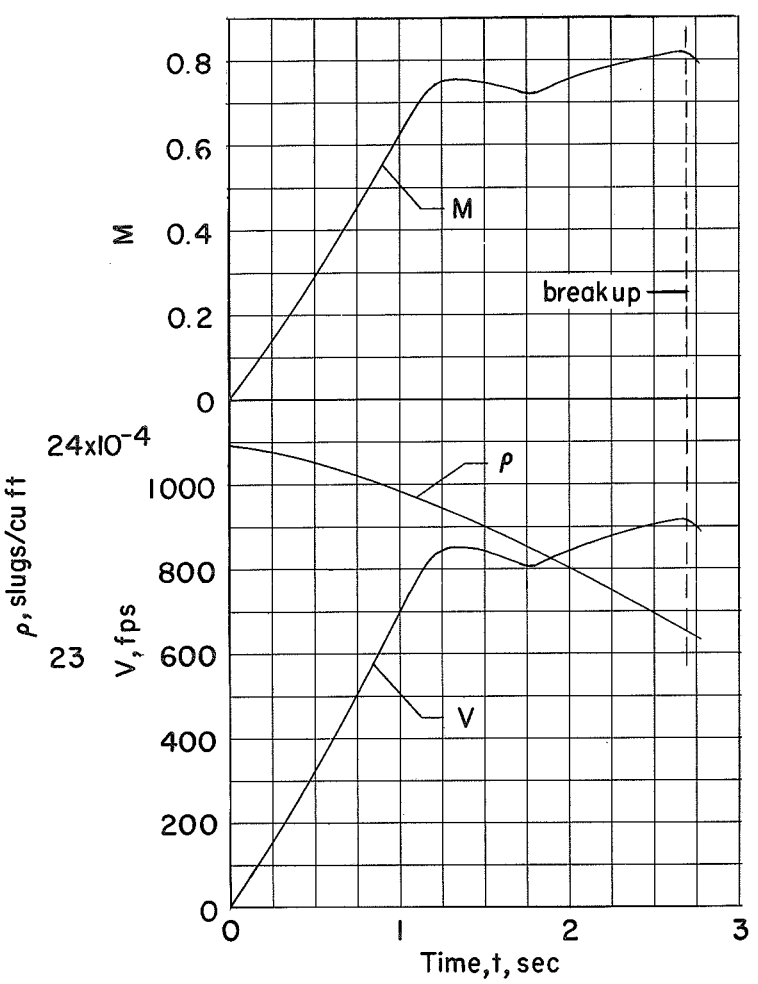

(a) Model 1.

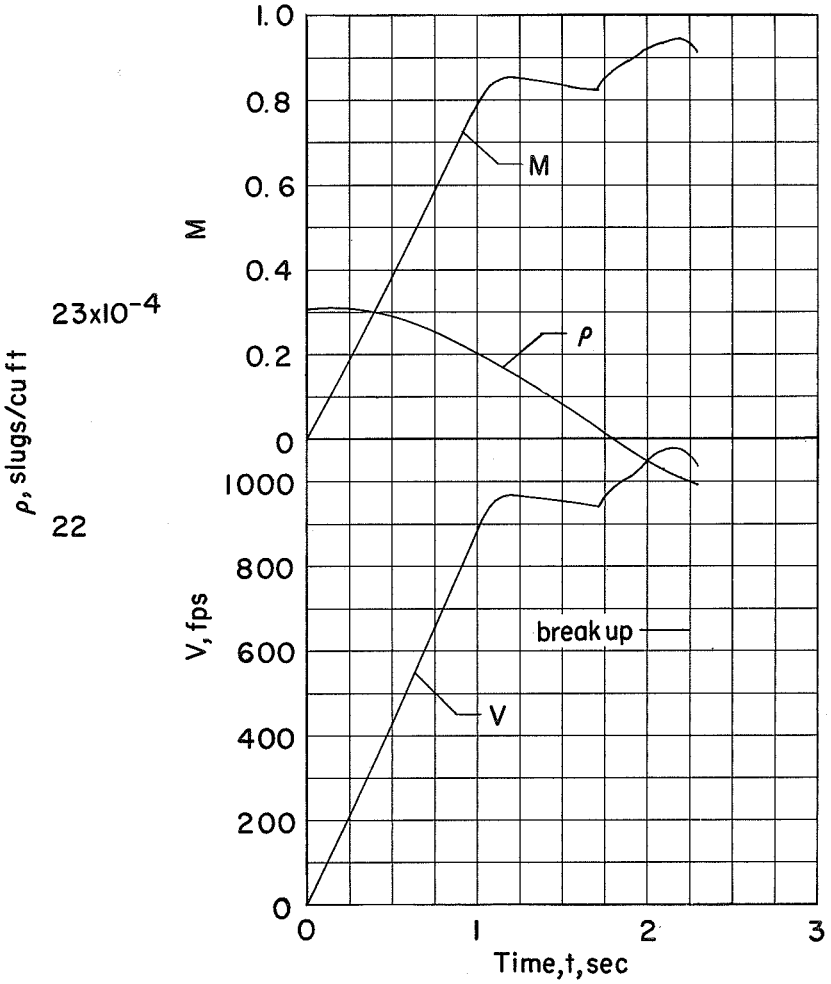

(b) Model 2.

Figure 6.- Time history showing Mach number, velocity, and atmospheric dneisty.

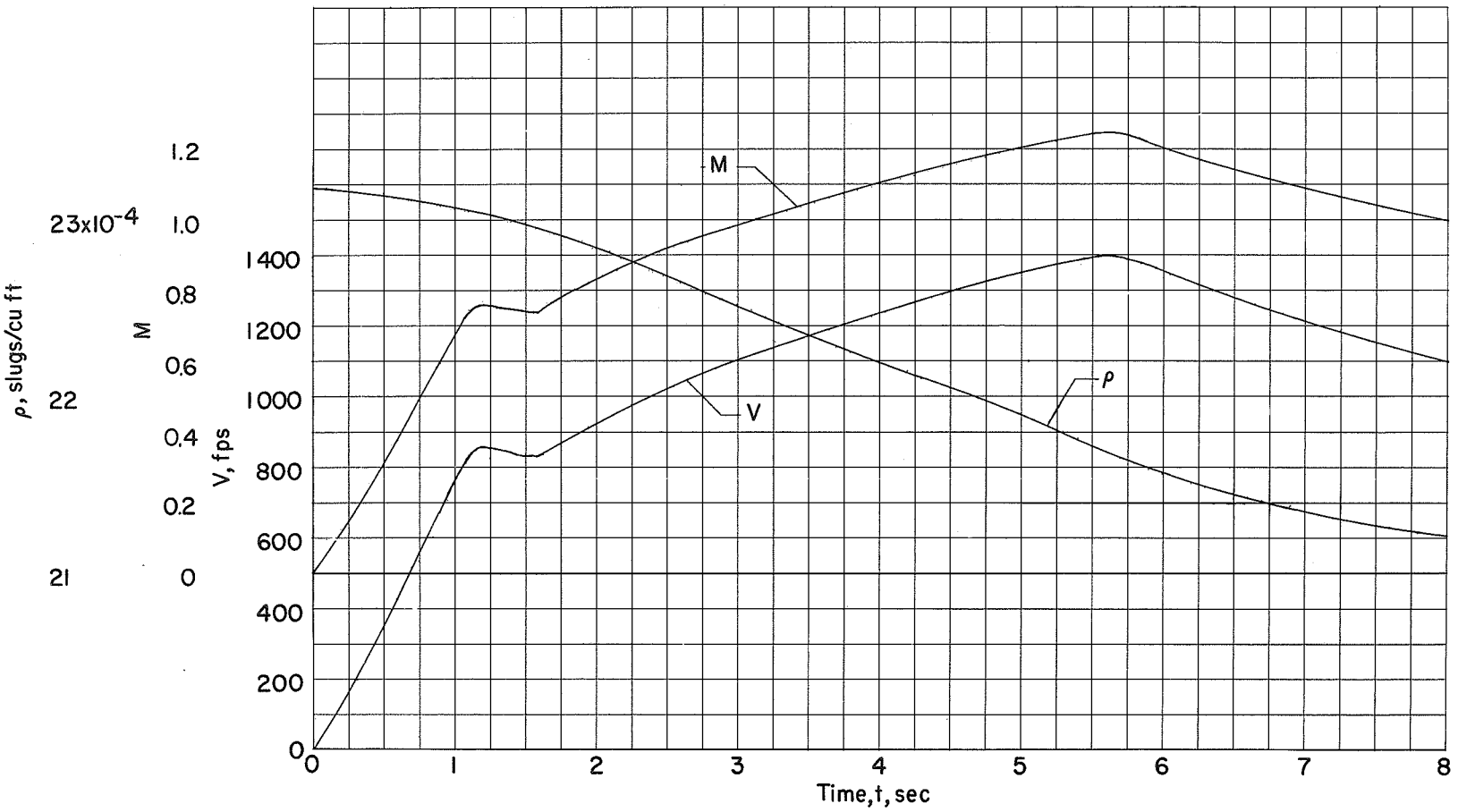

(c) Model 3.

Figure 6.- Continued.

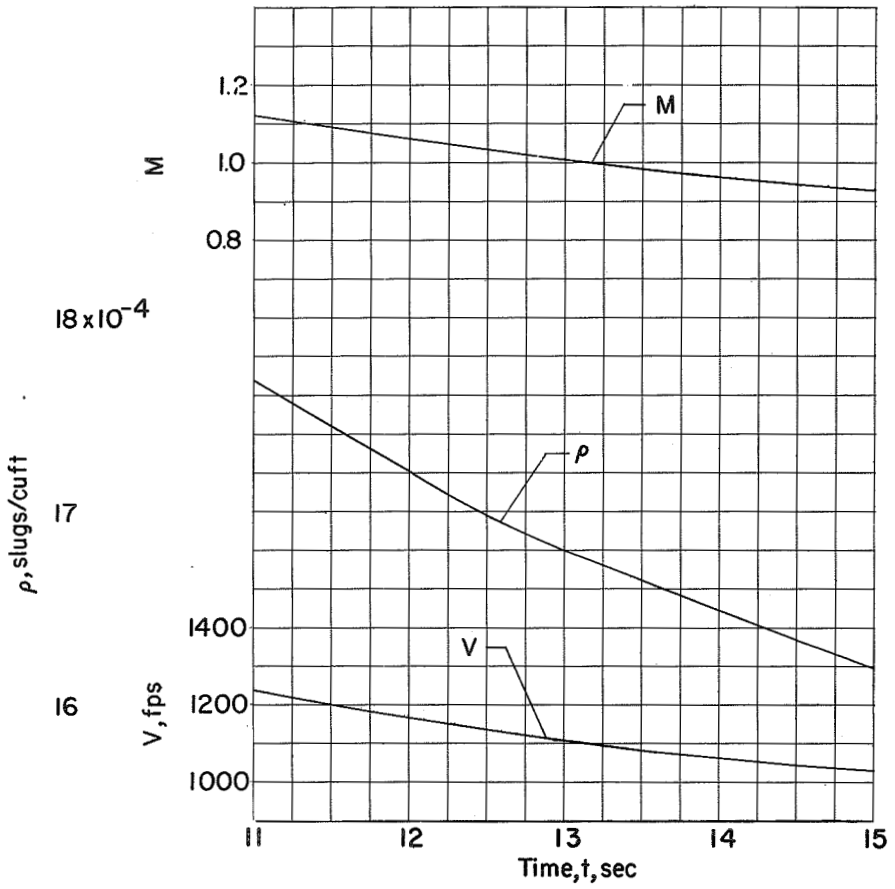

(d) Drag model 1.

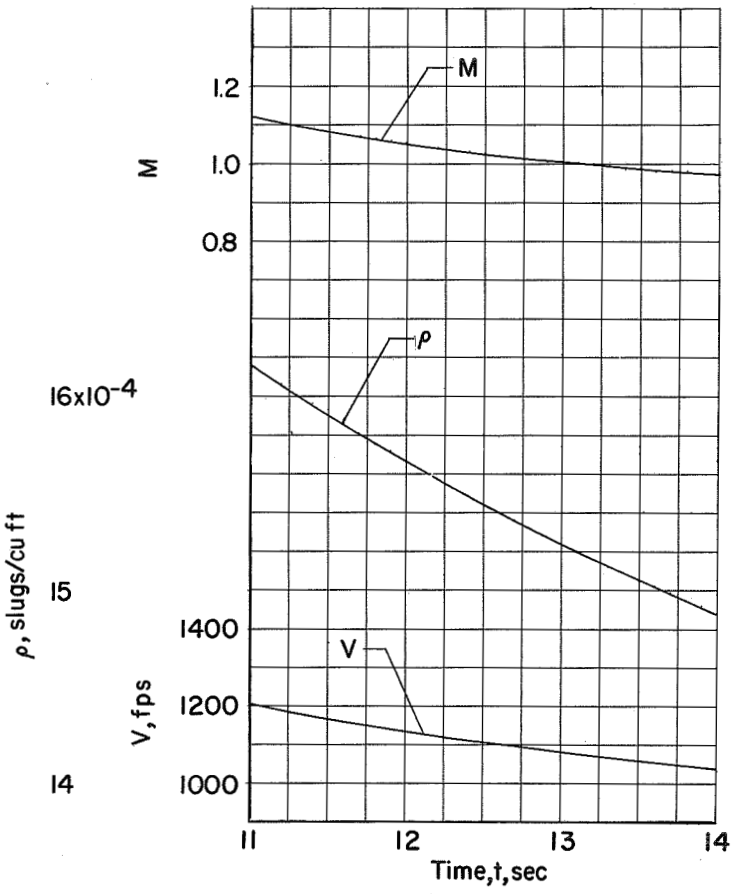

(e) Drag model 2.

Figure 6.- Concluded.

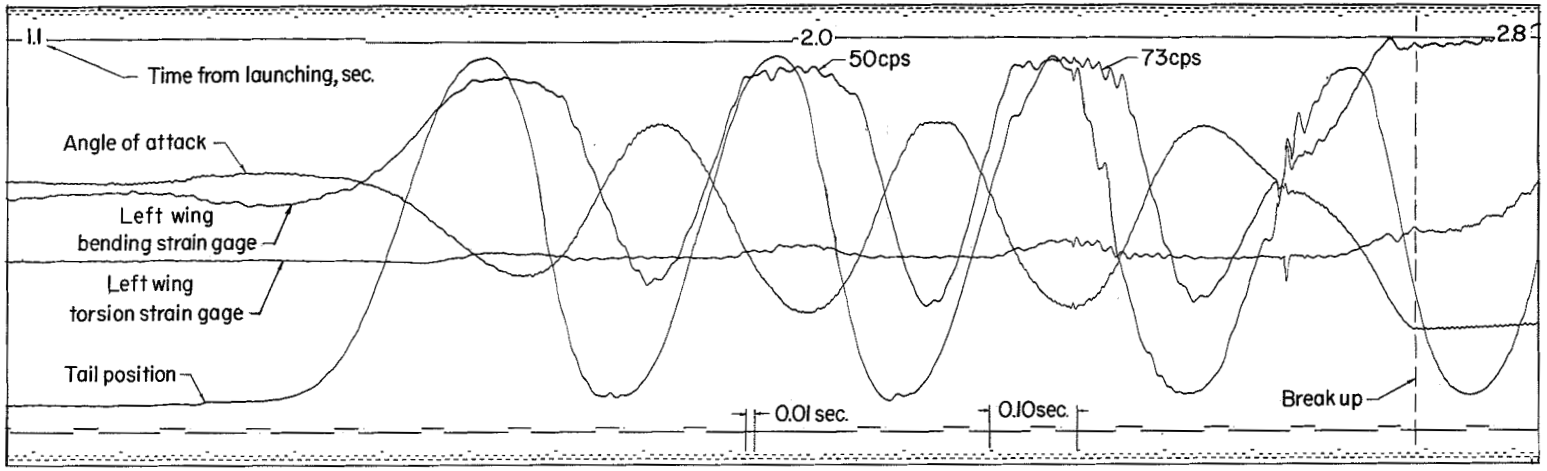

(a) Flutter model 1.

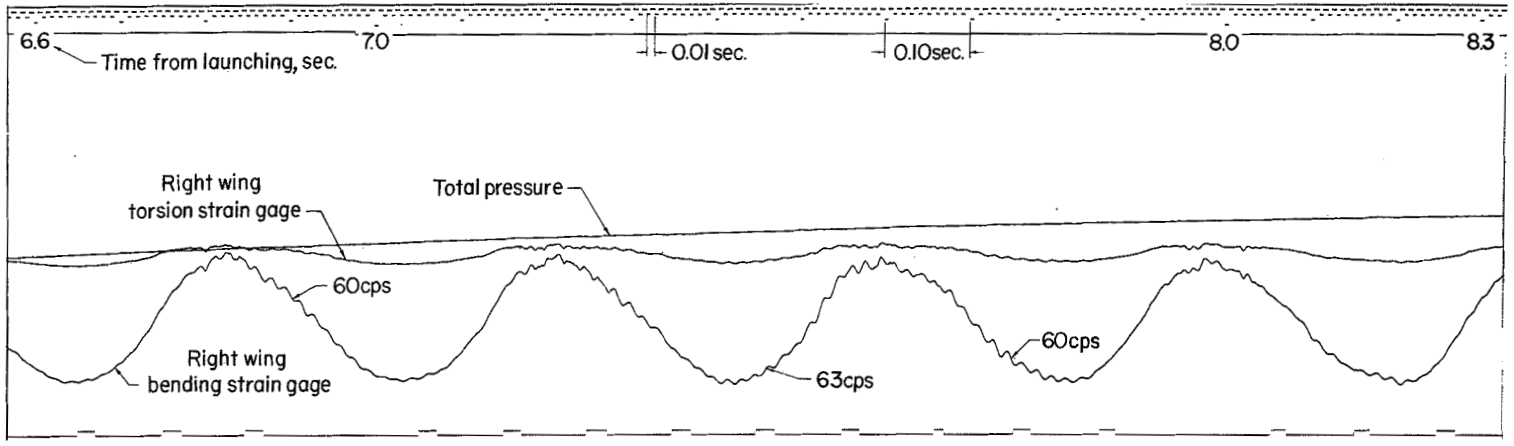

(b) Flutter model 3.

Figure 7.- Portions of the telemeter records.

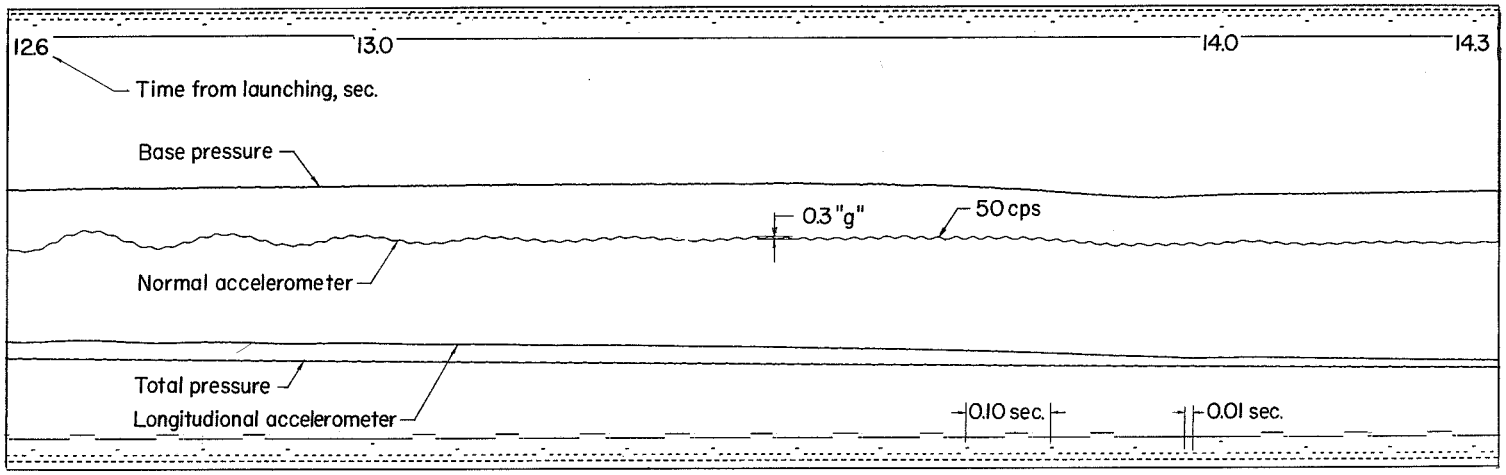

(c) Drag model 1.

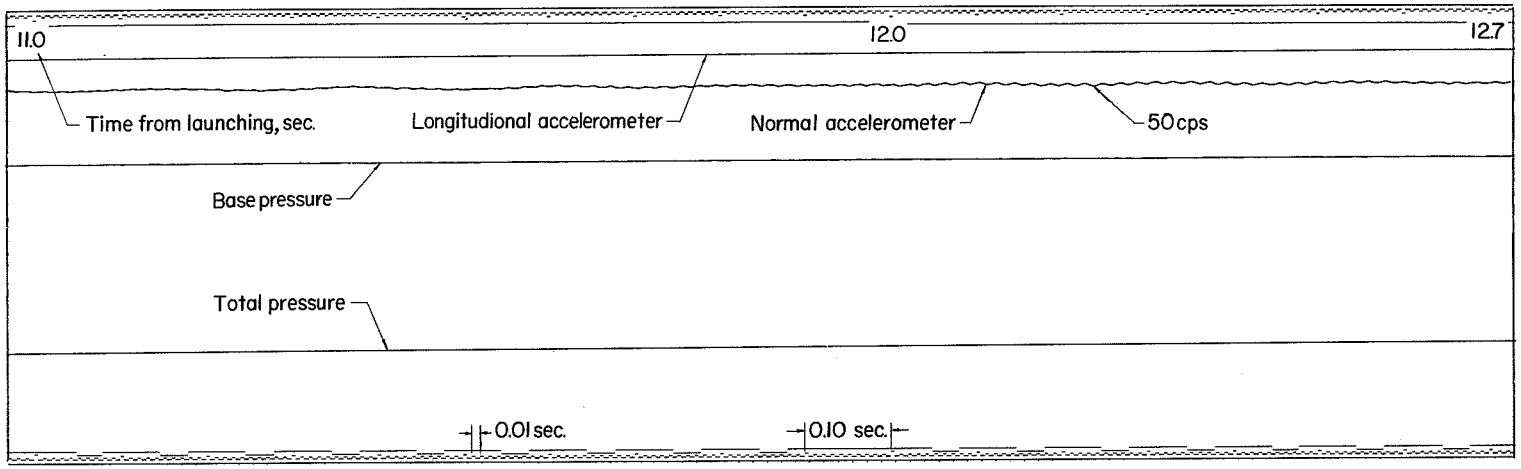

(d) Drag model 2.

Figure 7.- Concluded.

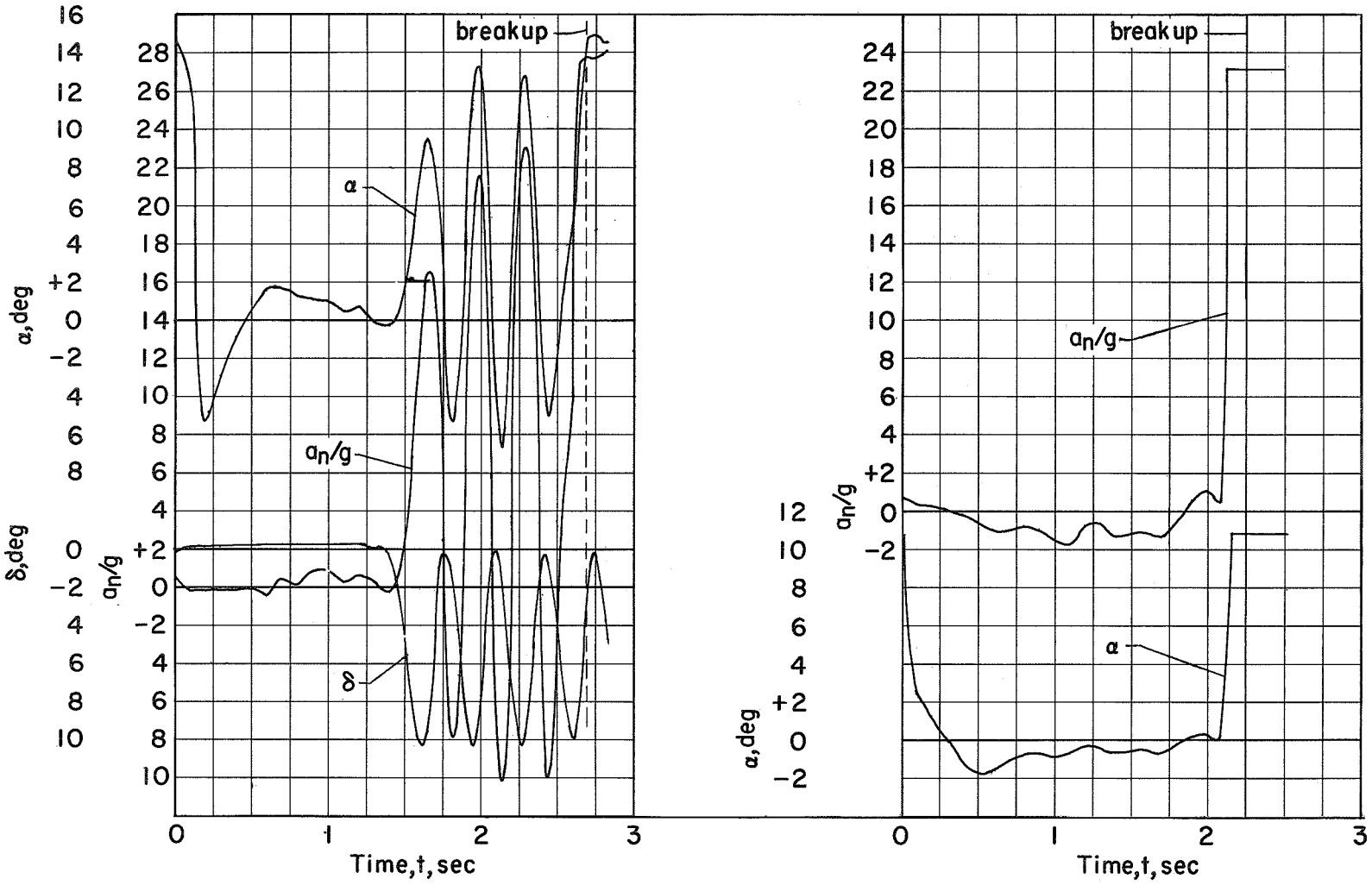

(a) Model 1. (b) Model 2.

Figure 8.- Reduction of data from the telemeter record.

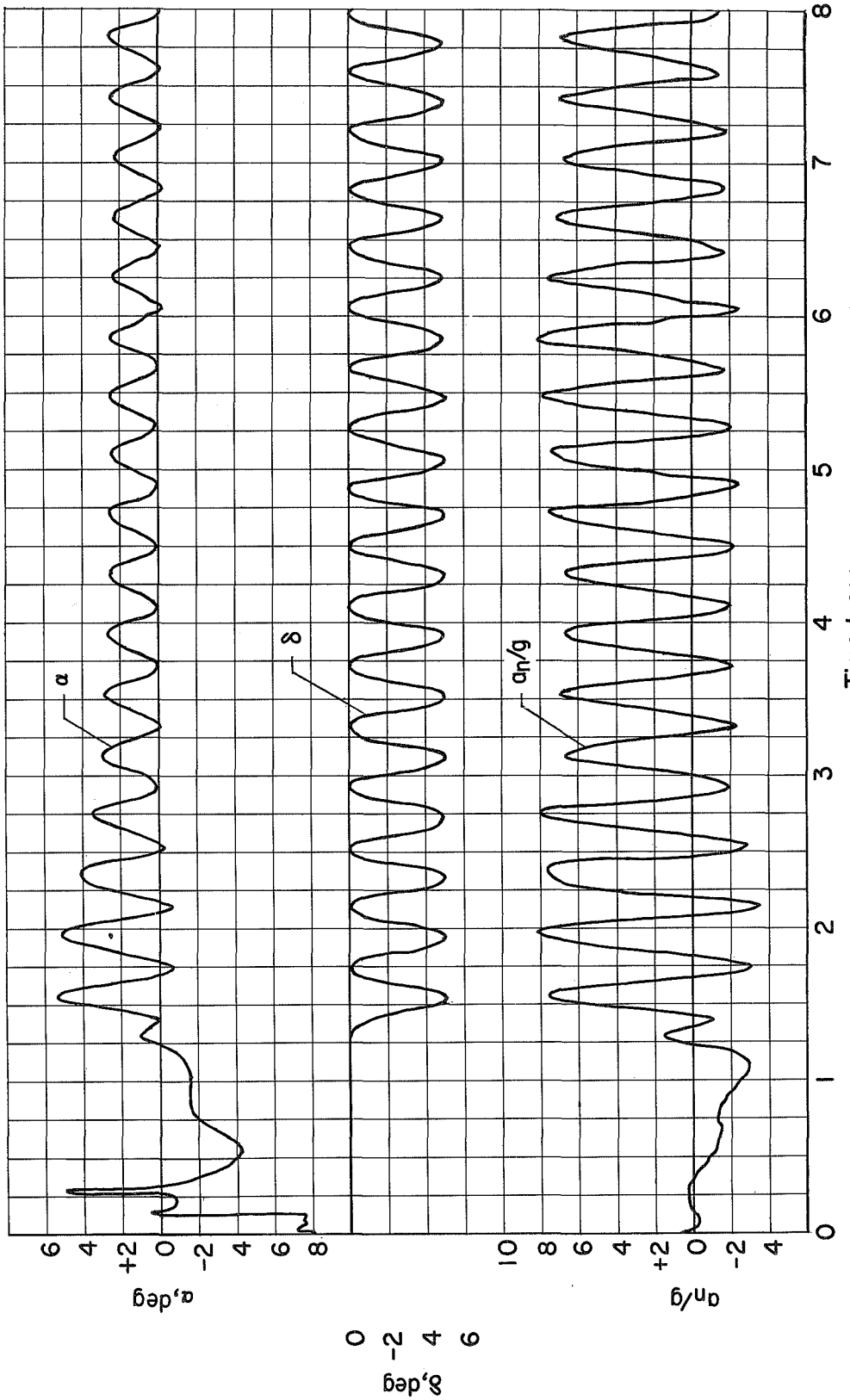

(c) Model 3.

Figure 8.- Concluded.